An Air–Sea Interaction Theory for Tropical Cyclones. Part I: Steady-State Maintenance

KERRY A. EMANUEL

Center for Meteorology and Physical Oceanography, Massachusetts Institute of Technology, Cambridge, MA 02139

(Manuscript received 19 February 1985, in final form 29 October 1985)

ABSTRACT

Observations and numerical simulations of tropical cyclones show that evaporation from the sea surface is essential to the development of reasonably intense storms. On the other hand, the CISK hypothesis, in the form originally advanced by Charney and Eliassen, holds that initial development results from the organized release of preexisting conditional instability. In this series of papers, we explore the relative importance of ambient conditional instability and air–sea latent and sensible heat transfer in both the development and maintenance of tropical cyclones using highly idealized models. In particular, we advance the hypothesis that the intensification and maintenance of tropical cyclones depend *exclusively* on self-induced heat transfer from the ocean. In this sense, these storms may be regarded as resulting from a finite amplitude air–sea interaction instability rather than from a linear instability involving ambient potential buoyancy. In the present paper, we attempt to show that reasonably intense cyclones may be maintained in a steady state without conditional instability of ambient air. In Part II we will demonstrate that weak but finite-amplitude axisymmetric disturbances may intensify in a conditionally neutral environment.

1. Introduction

Among the most spectacular and enigmatic features of the tropical atmosphere are the violently rotating circulations that occasionally form over the warmest parts of tropical oceans. These storms contrast greatly with the characteristic quiescence of the tropical atmosphere and have naturally been the subject of intense scientific interest for many centuries. A thorough review of the history and present status of research on tropical cyclones has been presented by Anthes (1982), while Ooyama (1982) has recently published an overview of the conceptual understanding of the development of these storms.

Beginning with the work of Ooyama (1969) there have been many relatively successful numerical simulations of tropical cyclones. These have advanced to the point where the effects of processes such as ice physics (Lord et al., 1984) and large-scale environmental asymmetries (Tuleya and Kurihara, 1981; DeMaria and Schubert, 1984) can be usefully examined. Despite the increasing sophistication of these models, the basic evolution and structure of the storms seem well captured by simple axisymmetric models such as Ooyama's. It should thus be possible to extract a basic conceptual understanding from these models together with observations.

Most numerical simulations begin with an atmosphere that is unstable with respect to undilute vertical displacements of low level air. In Ooyama's (1969) simulation, for example, air from the lowest of three model layers, if lifted to the uppermost layer, would be 10°C warmer than its environment in the initial condition of the model. In models with greater vertical resolution and more complicated treatments of moist convection it is common to use a mean tropical sounding, such as that of Jordan (1958), in the initial state. While such soundings are always unstable to undilute ascent of boundary layer air, it is not always clear whether entraining cumuli, either represented or explicitly simulated, will penetrate to significant altitudes.

All numerical simulations of tropical cyclones reveal the essential importance of latent (and perhaps sensible) heat flux from the sea surface, as proposed originally by Riehl (1954). In Ooyama's (1969) simulation, for example, only a weak vortex occurred when sea surface evaporation was turned off. The fact that any intensification occurs at all in the absence of sea–air heat flux is an indication that some convective available potential energy (CAPE) is present in the initial sounding. This increase in amplitude is generally ascribed to the mechanism proposed by Charney and Eliassen (1964) and by Ooyama (1964), whereby the moisture convergence in the boundary layer of a quasi-balanced vortex supports cumulus convection; it is important to note that this is a *linear* instability. Such an instability is particularly evident in simulations such as that of Anthes (1972), which develop a vortex from a resting initial condition with random perturbations added. Some nonlinear models, such as that of Carrier et al. (1971), are completely dependent on ambient CAPE.

Yet there are many grounds on which one may question the existence of such a linear instability in nature. While some CAPE certainly exists for undilute parcel ascent in the tropics, the ability of natural or simulated convection to realize this potential energy is

sensitive to details of turbulent mixing, microphysical interactions and other processes whose representation in numerical models is approximate. Indeed, the existence of a linear instability of the type envisioned by Charney and Eliassen (1964) would imply that weak tropical cyclones should be ubiquitous and not confined to maritime environments. In nature an asymmetric disturbance, such as an easterly wave, is almost always observed to precede the occurrence of tropical cyclones (e.g., see Anthes, 1982).

Our present purpose is to develop a somewhat different conceptual view of tropical cyclones. It is our hypothesis that tropical cyclones are developed and maintained against dissipation *entirely* by self-induced anomalous fluxes of moist enthalpy from the sea surface with virtually no contribution from preexisting CAPE. In this sense, the storms are taken to result from an air–sea interaction instability, which requires a finite amplitude initial disturbance. (In Part II we shall demonstrate the absence of a linear air–sea interaction instability in a conditionally neutral environment.) The instability relies on a simple feedback between radial temperature gradients that drive the circulation and radial gradients of sea–air heat transfer associated with gradients of surface wind speed. Cumulus convection is taken to redistribute heat acquired from the sea surface in such a way as to keep the environment locally neutral to slantwise moist convection in a manner consistent with the quasi-equilibrium hypothesis of Arakawa and Schubert (1974). In the idealized case of undilute parcel ascent, the ambient environment is taken to be conditionally neutral so that any kinetic energy generation is due to the in situ generation of CAPE rather than to ambient CAPE.

We emphasize that while this view departs in some ways from other conceptual views of tropical cyclones, the physics implied in this view are contained in virtually all contemporary numerical models which allow for convection and air–sea heat transfer.

In order to develop this hypothesis, we present an analytic but highly idealized nonlinear axisymmetric tropical cyclone model whose main distinguishing feature is the complete absence of any conditional instability to upright or slantwise moist convection. In Part I we show that such a model is capable of simulating intense steady-state storms. In Part II we shall use an extension of this model as well as a full primitive-equation numerical model to demonstrate that a weak but finite amplitude vortex may grow in a conditionally neutral environment.

2. A steady-state analytical model based on air–sea interaction[1]

We formulate here a highly idealized axisymmetric, steady-state model of a mature tropical cyclone. The model is based on the assumptions that flow above a well-mixed surface boundary layer is inviscid and thermodynamically reversible, that hydrostatic and gradient wind balance apply, and more particularly that *the thermal and kinematic structure of the tropical cyclone is such that the combined buoyant/centrifugal potential of boundary layer air is zero; i.e., that the vortex is neutral to slantwise moist convection.* There is considerable evidence (e.g., Emanuel, 1983, 1985) to suggest that baroclinic cyclones are often characterized by neutrality to slantwise convection, and we see no reason not to include the centrifugal as well as the buoyant component of convection in defining the state of neutrality. *This implies that boundary layer air is neutrally buoyant when lifted along surfaces of constant angular momentum* (Emanuel, 1983). This state is hardly distinguishable from a state of neutrality to upright convection in those parts of the cyclone where angular momentum surfaces are nearly vertical, but will be quite different in the uppermost portions where the angular momentum surfaces flair radially outward (e.g., see Schubert and Hack, 1983).

This assumption of slantwise neutrality is an idealization of the actual tropical cyclone, which precludes any role of ambient CAPE in the energetics of the vortex. This is consistent with Riehl's (1954) estimate that ambient CAPE contributes no more than about 15 mb to the hydrostatic pressure drop in cyclones. The assumption fails decidedly in the eyes of mature storms, which are observed to be very stable with respect to boundary layer air (e.g., see Jordan, 1957). It also breaks down in the region of descent in the outer portions of the storm, although the consequences of this are probably less serious since temperature perturbations are generally very small there (e.g., Frank, 1977). The assumptions of basic axisymmetry and gradient balance also break down in the outflow aloft.

The slantwise neutral assumption and reversible thermodynamics imply that above the boundary layer, the saturated equivalent potential temperature (θ_e^*) is uniform along surfaces of constant angular momentum and equal to the value of θ_e where the angular momentum surface intersects the boundary layer, within which θ_e is assumed to be well mixed in the vertical. The structure of the model is illustrated in Fig. 1. Here angular momentum per unit mass is defined

$$M \equiv rV + \frac{1}{2}fr^2, \tag{1}$$

where r is the radius from the cyclone center, V is the azimuthal velocity, and f is the Coriolis parameter (assumed constant).

It is important to note that above the boundary layer we are placing a restriction only on the distribution of saturated θ_e^* and not on θ_e itself; we are merely asserting that in the mature cyclone a saturated parcel originating in the boundary layer will experience neutral buoyancy when displaced along an angular momentum surface. While in a real tropical cyclone some positive buoyancy

[1] This model was developed contemporaneously with a similar model of D. K. Lilly (unpublished manuscript).

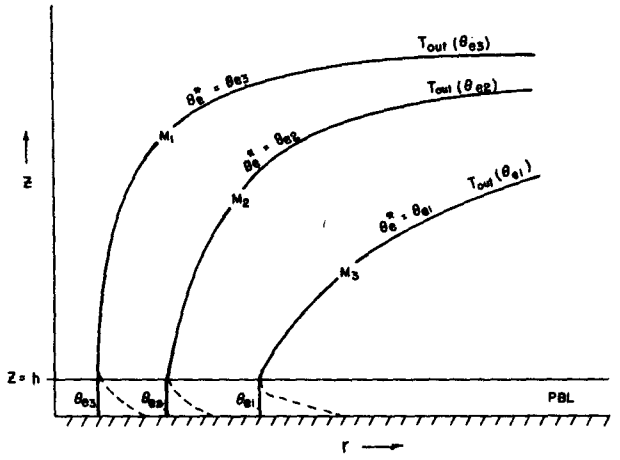

FIG. 1. Structure of the steady-state model. Curved lines above the planetary boundary layer (PBL) represent surfaces of constant angular momentum (M) and saturated equivalent potential temperature (θ_e^*). Solid lines in PBL show surfaces of constant θ_e while M is shown by dashed lines.

must be present to counter the effects of turbulent mixing, we regard this effect as small compared to the main source of energy for the cyclone.

a. Structure above the boundary layer

We now demonstrate that the assumptions of hydrostatic and gradient balance and slantwise neutrality above the boundary layer permit the development of certain exact analytic relationships between the wind and saturated entropy fields. In some ways, these resemble certain relationships developed by Thorpe (1985) for a dry, zero potential vorticity vortex; the present model may be characterized as having zero saturated moist potential vorticity.

In defining the neutrally buoyant state, we will neglect effects of latent heat of fusion and condensate loading. Under these assumptions, the hydrostatic and gradient wind relations may be written

$$\alpha \frac{\partial p}{\partial z} = -g, \tag{2}$$

$$\alpha \frac{\partial p}{\partial r} = \frac{V^2}{r} + fV = \frac{M^2}{r^3} - \frac{1}{4} f^2 r, \tag{3}$$

where g is the acceleration of gravity, p is the pressure and α is the specific volume. By virtue of (2), (3) may be written

$$g\left(\frac{\partial z}{\partial r}\right)_p = \frac{M^2}{r^3} - \frac{1}{4} f^2 r, \tag{4}$$

while (2) may be alternatively expressed by

$$g\left(\frac{\partial z}{\partial p}\right)_r = -\alpha. \tag{5}$$

Eliminating z between (4) and (5) results in a version of the thermal wind relation in radial coordinates:

$$\frac{1}{r^3}\left(\frac{\partial M^2}{\partial p}\right)_r = -\left(\frac{\partial \alpha}{\partial r}\right)_p. \tag{6}$$

If we assume reversible thermodynamics, α may be expressed as a function of pressure (p) and moist entropy (s^*) alone, by virtue of the equation of state and the first law of thermodynamics. Therefore,

$$\left(\frac{\partial \alpha}{\partial r}\right)_p = \left(\frac{\partial \alpha}{\partial s^*}\right)_p \left(\frac{\partial s^*}{\partial r}\right)_p. \tag{7}$$

It may be easily demonstrated from the first law of thermodynamics (see Appendix I) that $(\partial \alpha/\partial s^*)_p = (\partial T/\partial p)_{s^*}$. Using this in (7), we can rewrite (6) as

$$\frac{1}{r^3}\left(\frac{\partial M^2}{\partial p}\right)_r = -\left(\frac{\partial T}{\partial p}\right)_{s^*} \left(\frac{\partial s^*}{\partial r}\right)_p. \tag{8}$$

At this point we recall that the assumption that boundary layer parcels are neutrally buoyant along M surfaces is equivalent to the assumption that the (moist) entropy of lifted parcels equals the saturated entropy of the environment. This implies that the saturated moist entropy does not vary along M surfaces (neglecting the effects of condensate loading and latent heat of fusion). Since s^* is then a function of M alone, (8) may be written

$$\frac{1}{r^3}\left(\frac{\partial M^2}{\partial p}\right)_r = -\left(\frac{\partial T}{\partial p}\right)_{s^*} \frac{ds^*}{dM} \left(\frac{\partial M}{\partial r}\right)_p. \tag{9}$$

Dividing (9) through by $\partial M/\partial r$ yields an expression for the slope of M (or s^*) surfaces:

$$\left(\frac{\partial r}{\partial p}\right)_M = \frac{r^3}{2M} \frac{ds^*}{dM} \left(\frac{\partial T}{\partial p}\right)_{s^*}. \tag{10}$$

If (10) is integrated upward along M (or s^*) surfaces, the result is

$$r^2|_M = \frac{M}{-\dfrac{ds^*}{dM}[T - T_{out}(s^*)]}, \tag{11}$$

where T_{out} is an integration constant that may be a function of s^* (or M). Inspection of (11) shows that T_{out} may be interpreted as the "outflow temperature," the temperature the air has along M surfaces as they flare out to very large radii. The relation (11) yields the shape (in r–T space) of angular momentum and entropy surfaces, and is a cornerstone of the present model. Along the top of the boundary layer, (11) may be written

$$-r^2 \frac{ds^*}{dM}(T_B - T_{out}) = M \quad \text{at} \quad z = h, \tag{12}$$

where T_B is the absolute temperature at the top of the boundary layer ($z = h$). Multiplying the above by $\partial M/\partial r$ results in

$$-r^2 \frac{\partial s^*}{\partial r}(T_B - T_{\text{out}}) = \frac{1}{2}\frac{\partial M^2}{\partial r} \quad \text{at} \quad z = h. \tag{13}$$

A relationship between pressure and moist entropy may now be derived from (13) using the gradient wind relationship (3). First recall that at the top of the boundary layer, saturated moist entropy is assumed to equal the actual moist entropy of the boundary layer:

$$s^* = C_p \ln\theta_e \quad \text{at} \quad z = h. \tag{14}$$

Also, for convenience of notation, we use the Exner function in place of pressure:

$$\pi = (p/p_0)^{R/C_p}. \tag{15}$$

Using (15), the gradient wind relationship (3) may be written

$$M^2 = r^3\left[C_p T_B \frac{\partial \ln\pi}{\partial r} + \frac{1}{4}f^2 r\right]. \tag{16}$$

We now substitute (16) and (14) into (13) to derive a relationship between θ_e and π at the top of the boundary layer. In doing so, we take T_B to be constant as is generally observed (e.g., see Frank, 1977). The resulting expression may be written

$$-\frac{T_B - T_{\text{out}}}{T_B}\frac{\partial \ln\theta_e}{\partial r} = \frac{\partial \ln\pi}{\partial r} + \frac{1}{2}\frac{\partial}{\partial r}\left(r\frac{\partial \ln\pi}{\partial r}\right) + \frac{1}{2}\frac{f^2 r}{C_p T_B} \quad \text{at} \quad z = h. \tag{17}$$

This may be directly integrated once in r to yield

$$-\frac{T_B - \bar{T}_{\text{out}}}{T_B}\ln\frac{\theta_e}{\theta_{ea}} = \ln(\pi/\pi_a) + \frac{1}{2}r\frac{\partial \ln\pi}{\partial r} + \frac{1}{4}\frac{f^2}{C_p T_B}(r^2 - r_0^2) \quad \text{at} \quad z = h, \tag{18}$$

where π_a is the ambient value of π at $z = h$ and r_0^2 is an integration constant chosen in such a way that θ_e equals its ambient value θ_{ea} and both $\ln\pi/\pi_a$ and its radial gradient vanish at $r = r_0$. Hence r_0 may be interpreted as the radial extent of the storm near sea level. The value of $\bar{T}_{\text{out}}$ is an average outflow temperature weighted with the saturated moist entropy of the outflow angular momentum surfaces:

$$\bar{T}_{\text{out}} \equiv \frac{1}{\ln\theta_e^*/\theta_{ea}}\int_{\ln\theta_{ea}}^{\ln\theta_e} T_{\text{out}}\, d\ln\theta_e^*, \tag{19}$$

where it should be remembered that θ_e^* along angular momentum surfaces is taken to equal θ_e where these surfaces intersect the boundary layer.

The integration constant r_0 may be taken to represent the outermost closed isobar of an axisymmetric storm. Its value can only be determined through a time-dependent model; in the present steady model it must be arbitrarily specified. (In section 2c, however, we show that closing the system with a boundary layer model leads to a specific relationship between r_0 and the radius of maximum winds.) It is possible to show that r_0^2 is directly proportional to the areal average moist entropy of the boundary layer. To do this, we first rewrite (18)

$$\frac{d}{dr}\left[r^2 \ln\frac{\pi}{\pi_a}\right] = -2r\frac{T_B - \bar{T}_{\text{out}}}{T_B}\ln\frac{\theta_e}{\theta_{ea}} + \frac{1}{2}\frac{f^2}{C_p T_B}[r_0^2 r - r^3].$$

Integrating the above outward from $r = 0$ results in

$$\ln\frac{\pi}{\pi_a} = -\frac{2}{r^2}\int_0^r \frac{T_B - \bar{T}_{\text{out}}}{T_B}\ln\frac{\theta_e}{\theta_{ea}}\, r\, dr + \frac{1}{4}\frac{f^2}{C_p T_B}\left(r_0^2 - \frac{1}{2}r^2\right).$$

But since by definition $\pi = \pi_a$ at $r = r_0$, the above implies that

$$r_0^2 = \frac{16 C_p T_B}{f^2}\frac{1}{r_0^2}\int_0^{r_0}\frac{T_B - \bar{T}_{\text{out}}}{T_B}\ln\frac{\theta_e}{\theta_{ea}}\, r\, dr. \tag{20}$$

Thus the geometric area covered by the storm is related to its areal-average boundary layer moist entropy surfeit.

An alternative derivation of (18) in terms of total storm energetics is provided in section 3. We note here that since (18) implies that V goes to zero at $r = r_0$, negative relative vorticity exists in the outer regions of the cyclone and this will generally be accompanied by Ekman flow into the boundary layer. Under these conditions one would expect the assumption that slantwise convection maintains a neutral lapse rate breaks down in this region, as noted previously.

At this point we note that the relationships derived thus far are approximately valid in the eye to the extent that the eye is in solid body rotation at all levels. This is because surfaces of constant s^* and M are approximately parallel under the circumstance that the eye is in solid body rotation at each level and is bounded on the outside by an M surface that coincides with an s^* surface. This is shown in Appendix II. It will not necessarily be true, however, that s^* above the boundary layer coincides with s in the boundary layer within the eye.

b. Central pressure

In order to complete the model, a second relationship between pressure and θ_e in the boundary layer must be obtained from a model of the boundary layer. This will be attempted in section 2c. However, the relationship between pressure and θ_e expressed by (18) constitutes a powerful constraint on the structure of the

steady axisymmetric tropical cyclone. Note that at the storm's center, (18) implies that

$$\ln\frac{\pi_c}{\pi_a} = -\frac{T_B - \bar{T}_{\text{out}}}{T_B}\ln\frac{\theta_{ec}}{\theta_{ea}} + \frac{1}{4}\frac{f^2 r_0^2}{C_p T_B}, \quad (21)$$

where the subscript c denotes the value at the storm center. This shows that the pressure deficit may be expected to be weaker in geometrically larger storms, although substitution of numerical values shows that the effect only becomes noticeable when $r_0 \gtrsim 500$ km. Also notice that the natural length scale that appears in (21)

$$L \sim \sqrt{C_p T_B}/f,$$

differs somewhat from the classical definition of the deformation radius, although it may be expressed as the potential temperature scale height $C_p T_B/g$ multiplied by the buoyancy frequency of an isothermal atmosphere with temperature T_B and divided by f. Its typical magnitude in the tropics is about 10 000 km.

Since π_c/π_a and θ_{ec}/θ_{ea} differ only slightly from unity, (21) implies a nearly linear relationship between pressure deficit and θ_e^* surfeit in the storm center. Expanding the natural logarithms in (21) and using the definition of π (15),

$$p_c' \approx -\frac{C_p}{R}p_a\frac{T_B - \bar{T}_{\text{out}}}{T_B}\frac{\theta_{ec}^{*\prime}}{\theta_{ea}},$$

where the primes denote departures from the base state values and p_a is the ambient pressure at $z = h$. Assuming that p_c'/p_a is approximately equal to p_{cs}'/p_0, where p_{cs}' is the ambient surface pressure, and using $\theta_{ea} = 345$ K, $p_0 = 1015$ mb, $T_B = 295$ K and $\bar{T}_{\text{out}} = 200$ K, the above is

$$p_{cs}' \approx 3.3\theta_{ec}^{*\prime} \quad \text{at} \quad z = 0, \quad (22)$$

where p_{cs}' and θ_{ec}' are expressed in millibars and degrees Kelvin, respectively. This relationship may be compared to a similar one derived empirically by Riehl (1963) and from the hydrostatic equation by Malkus and Riehl (1960):

$$p' = -2.6\theta_e'.$$

This second relation pertains to the surface pressure and θ_e at the base of the *eye wall,* whereas (22) relates the central pressure to θ_e^* at the storm center. The hydrostatic derivation by Malkus and Riehl differs from the derivation of (22) in that the former must assume a level of vanishing pressure perturbation while in the present case we need only evaluate the outflow temperature at large radii; the vertical distribution of pressure is then determined by the constraints of gradient and hydrostatic balance and slantwise neutrality. Yet it should be remembered that, in the eye, θ_e^* above the boundary layer may differ from both θ_e^* and θ_e within the boundary layer so that the former should be used in evaluating (22).

We can now show that (21) implies that an inward increase in surface relative humidity is necessary in a tropical cyclone, at least in the absence of strong subsidence in the eye, in which case θ_e^* above the boundary layer may exceed θ_e within the boundary layer. Assuming that θ_e is vertically uniform from the top of the mixed layer to the top of the surface layer and using the definition of θ_e,

$$\ln\theta_e|_{z=h} = \ln\theta_{es} = \ln T_s - \ln\pi_s + \left(\frac{Lq}{C_p T}\right)_s,$$

where the subscript s denotes the value at the top of the surface layer, L is the heat of vaporization and q is the mixing ratio. Provided T_s is constant we can write

$$\ln\frac{\theta_e}{\theta_{ea}}\bigg|_{z=h} = \ln\frac{\theta_{es}}{\theta_{ea}} = -\ln\pi_s + \frac{L}{C_p T_s}(q - q_a)_s,$$

where q_a is the ambient mixing ratio at the top of the surface layer. Rewriting the above in terms of relative humidity,

$$\ln\frac{\theta_e}{\theta_{ea}}\bigg|_{z=h} = -\ln\pi_s + \frac{L}{C_p T_s}(q^*\text{RH} - q_a^*\text{RH}_a)_s, \quad (23)$$

where RH denotes relative humidity and the asterisk refers to the saturated values. The saturation specific humidity at constant temperature may be expressed

$$q^* = q_a^*\frac{p_0}{p} = q_a^*\pi_s^{-C_p/R} \approx q_a^*\left[1 - \frac{C_p}{R}\ln\pi_s\right]. \quad (24)$$

The last relation is obtained since $\ln\pi_s$ is small. Substituting (24) in (23) results in a relationship between θ_e, pressure and relative humidity at the top of the surface layer:

$$\ln\frac{\theta_e}{\theta_{ea}} \approx -\ln\pi_s\left[1 + \frac{Lq_a^*\text{RH}_s}{RT_s}\right] + \frac{Lq_a^*}{C_p T_s}(\text{RH} - \text{RH}_a)_s. \quad (25)$$

Finally, we note that since the absolute temperature of the boundary layer is nearly constant with radius, the hydrostatic equation may be used to demonstrate that

$$\left(\ln\frac{\pi}{\pi_a}\right)\bigg|_{z=h} = \ln\pi_s.$$

Using the above and (25) together with (21) results in a relationship between central surface pressure and the increase in surface relative humidity between the core and the ambient environment:

$$\ln\pi_{cs} \approx \frac{-\left(\frac{T_B - \bar{T}_{\text{out}}}{T_B}\right)\frac{Lq_a^*}{C_p T_s}(\text{RH}_c - \text{RH}_a)_s + \frac{1}{4}\frac{f^2 r_0^2}{C_p T_B}}{1 - \left(\frac{T_B - \bar{T}_{\text{out}}}{T_B}\right)\left(1 + \frac{Lq_a^*\text{RH}_{cs}}{RT_s}\right)}. \quad (26)$$

This expression for the central pressure shows that *a transfer of heat above and beyond that associated with isothermal expansion is needed to sustain a tropical cyclone. This extra-isothermal transport is reflected by an inward increase of relative humidity.* The term associated with isothermal sensible and latent heat fluxes appears in the denominator of (26). A remarkable inference from this model is that for a sufficiently large difference between inflow and outflow absolute temperature and/or sufficiently large absolute vapor content of boundary layer air, the right-hand side of (26) becomes very large and negative and the surface pressure therefore becomes quite small. [The pressure never goes to zero if the exact pressure dependence of q_s is used rather than the approximation given by (24).] Even for extreme values of parameters found on earth this does not happen, but, in principle, hurricanes might be extremely intense were the sea-surface temperature significantly higher or the lower stratosphere significantly colder than at present. We do not believe that this qualitative conclusion depends on the few simplifying assumptions made in constructing this model.

An upper bound on the surface pressure deficit may be found by setting the central surface humidity to 100% in (26). While this is probably an overestimate of the actual humidity in the eyes of even intense hurricanes (e.g., Frank, 1977), the error works to compensate the neglect of subsidence warming in the eye, though there is no apparent reason to believe this compensation should be exact. The minimum central pressure thus calculated is shown as a function of surface ambient air temperature and mean outflow temperature in Fig. 2. Here we have assumed that the undisturbed surface pressure is 1015 mb, that the ambient relative humidity is 80%, and that the temperature at the top of the boundary layer is 5°C less than the surface temperature. Also, we have used f at 20 degrees latitude and taken r_0 to be 500 km, although for these values the last term in the numerator of (26) has a negligible effect on the solution except at very low ambient surface air temperatures.

It is evident from Fig. 2 that the solutions exhibit great sensitivity to surface air temperature and are somewhat sensitive to outflow temperature as well. The range of predicted minimum sea level pressures is reasonable, although no cutoff at small air temperatures occurs. It should be noted that the ordinate in Fig. 2 is air temperature rather than sea surface temperature; Riehl (1954) and others suggest that the ambient air temperature is usually between 1° and 2°C less than sea surface temperature in tropical cyclones, though this may reflect wetting of temperature sensors. Notice that the maximum potential intensity of cyclones begins to increase quite rapidly with surface air temperature when the latter exceeds about 28°C. Since tropical cyclones significantly reduce sea surface temperatures, due principally to upwelling (Price, 1981), it may be that this effect acts as a natural brake on tropical sea surface temperatures in certain locations and times.

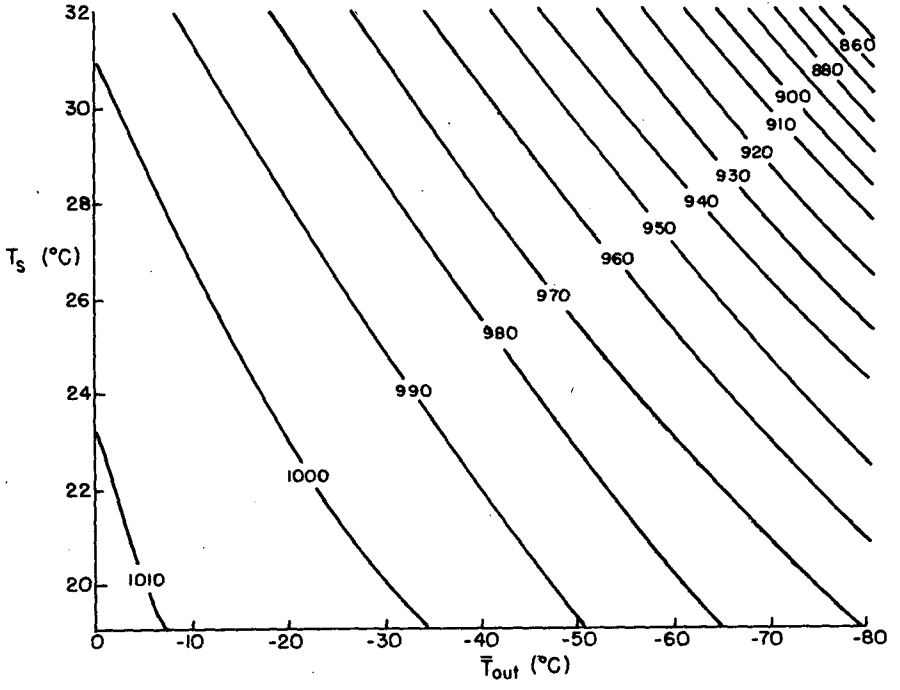

FIG. 2. Minimum attainable central surface pressure (mb) computed from (26) as a function of surface air temperature (T_s) and weighted mean outflow temperature ($\bar{T}_{out}$) assuming an ambient surface pressure of 1015 mb, ambient surface relative humidity of 80%, f evaluated at 20 degrees latitude, and r_0 = 500 km.

It is our contention that the observed absence of tropical cyclone *formation* when the sea surface temperature (SST) is less than 26°C is due to the absence of extensive deep conditional instability or neutrality over those parts of the ocean with SSTs less than this critical value. As is apparent in Fig. 2, outflow temperatures at least as low as −20°C must be achieved for disturbances to attain tropical storm strength for $T_s < 26$°C. This implies that the (undisturbed) conditionally neutral layer must extend up to at least the height of about the −20°C isothermal surface for tropical storm development to occur. As a rough measure of the degree of conditional instability or stability up to about the height of the −20°C surface, we examine the temperature surpluses at 300 mb of parcels lifted moist adiabatically from 1000 mb using July and January mean conditions at about 40 rawinsonde stations located on islands or ships. For this purpose we use atmospheric data and sea surface temperatures from Newell et al. (1972). Figure 3 shows the difference between the temperature of a parcel lifted adiabatically from 1000 mb to 300 mb and the ambient 300 mb temperature, plotted as a function of sea surface temperature. With only one exception, deep conditional neutrality is absent when the sea surface temperature is less than 25°C and most unstable cases are associated with sea surface temperatures exceeding 26°C. If the dilution of convective updrafts is accounted for, then effective neutrality to convective ascent is achieved only for appreciably positive values of the lifted index and here it is clearly evident that, as a purely statistical conclusion, sea surface temperatures must exceed 26 or 27°C for deep conditional neutrality.

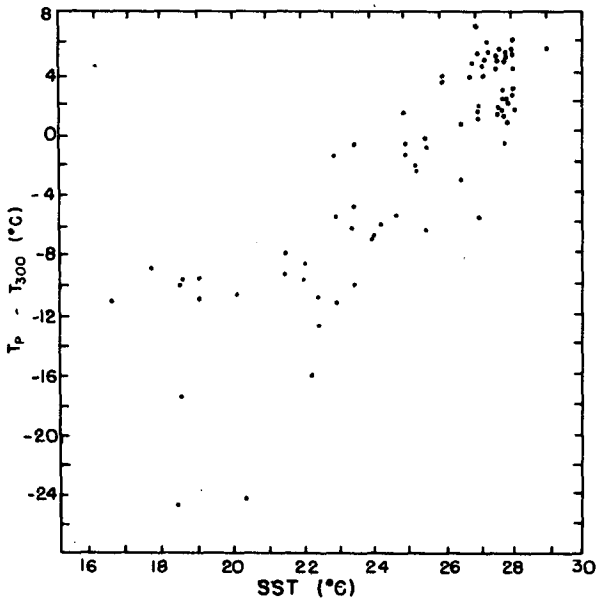

FIG. 3. Difference between temperature of parcel reversibly lifted from the boundary layer (T_p) and ambient 300 mb temperature (T_{300}) as a function of sea surface temperature computed using island and ship rawinsonde climatology.

The intensity achieved by mature tropical cyclones depends even more directly on sea surface temperature, as indicated in Fig. 2. In order to estimate the minimum central pressure attainable by tropical cyclones under normal oceanic and atmospheric conditions, we use surface and standard level data averaged for the month of September 1979, obtained from the National Oceanographic and Atmospheric Administrations's Environmental Data and Information Service, and mean September sea surface temperatures from Reynolds (1982). Minimum sea level central pressures over the globe were estimated from (26) using the following procedure. First, the monthly mean standard pressure level station temperatures were subjectively analyzed at the various levels over the oceans. Surface relative humidities were similarly analyzed using island and some coastal monthly mean surface observations. As these observations appeared to be quite noisy, the surface relative humidity was assumed to be 78% except in certain locations where lower humidity was definitely indicated. Oceanic surface air temperatures were assumed to equal the sea surface temperature. The mean outflow temperature $\bar{T}_{out}$ was then estimated by averaging T at equal intervals of 2.5°C in θ_e^* along vertical soundings constructed from the analyzed pressure level temperature data. In this averaging, the lowest value of θ_e^* is the value of θ_e at the surface, while the highest value is the value of θ_e representing saturation at sea surface temperature and at the computed central surface pressure. Since the latter is the result of the calculations, the upper limit of θ_e must be calculated iteratively. Finally, T_B was estimated to be 5°C lower than the sea surface temperature (the results are relatively insensitive to this value), r_0 was set at 500 Km, and the ambient surface pressure was fixed at 1015 mb. The minimum attainable central pressure was obtained by taking the central surface relative humidity to be 100%.

Figure 4 shows the results of the calculations; these results may be interpreted as the minimum central pressures attainable by tropical cyclones under climatological mean September conditions. In interpreting Fig. 4, it should be remembered that tropical cyclones will not generally form within 5° latitude of the Equator and that high sea surface temperatures may not persist in the presence of a strong tropical cyclone, particularly if the warm water is contained only in a relatively shallow layer (Price, 1981). Lower central pressures will be obtained if conditions depart from these climatological conditions or if subsidence in the eye produces values of θ_e^* that are substantially higher than saturated θ_e^* at sea level.

Aside from the absence of an equatorial minimum, the distributions shown in Fig. 4 are in reasonable accord with the known September statistics on tropical cyclones and show the major storm regions of the western North Pacific, the East Pacific off Central Mexico, the Caribbean and Gulf of Mexico, and the Bay of Bengal. The values of the lowest attainable cen-

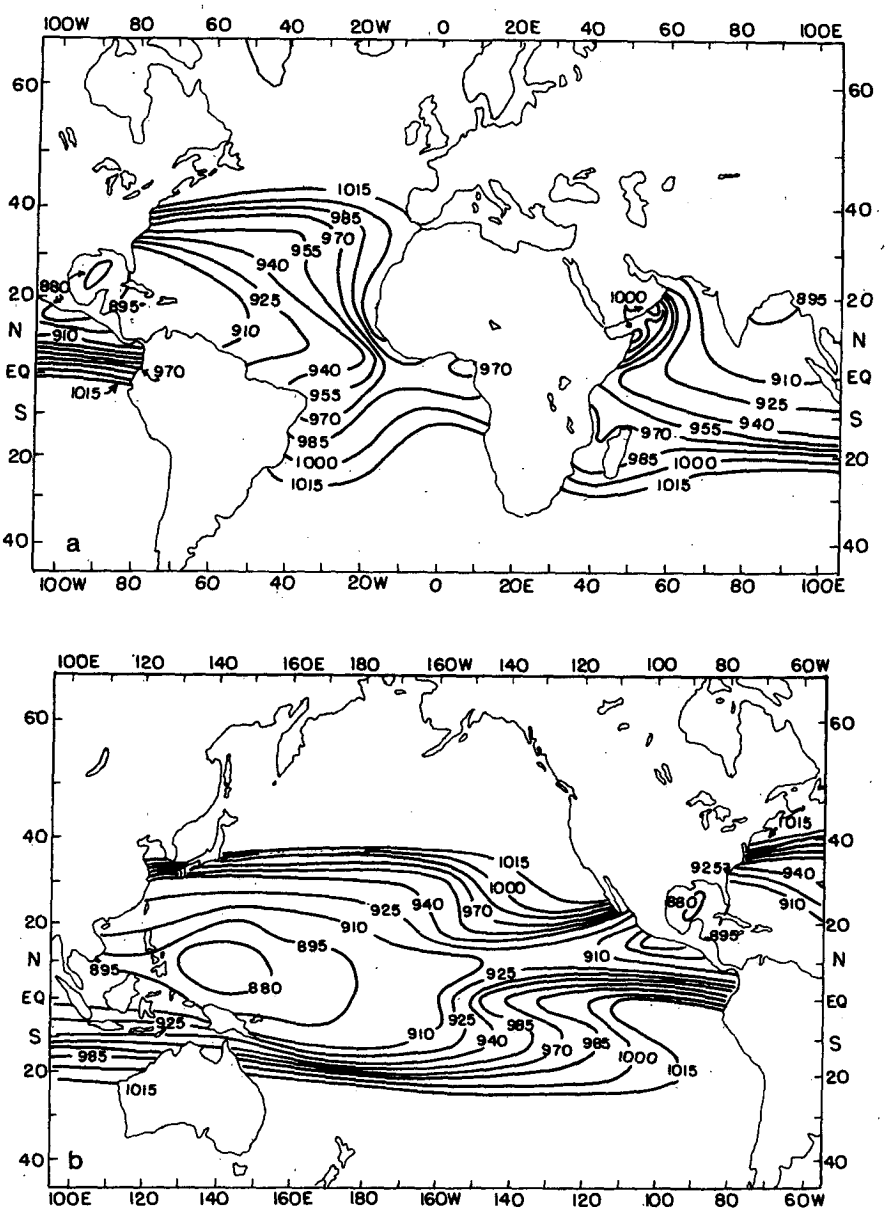

FIG. 4. Minimum attainable surface central pressure (mb) in September (a) for Atlantic and Indian Oceans and (b) for Pacific Ocean. See text for explanation.

tral pressures are reasonable for the time of year, although lower pressures are presumably possible where conditions depart from the standard assumed here.

c. *The boundary layer*

In the previous section it was shown that the three assumptions of hydrostatic and gradient wind balance and neutrality to slantwise moist convection from the boundary layer place severe restrictions on the structure and magnitude of the steady axisymmetric vortex. It is well known from other balance theories (e.g., Thorpe, 1985) that knowledge of the interior distribution of potential vorticity together with the distribution of potential temperature along the boundaries is sufficient to determine the entire solution. (This has become known as the "invertibility principle," Hoskins et al., 1985.) In the present case we have effectively specified the internal distribution of saturated equivalent potential vorticity, which is everywhere zero since the vorticity vector is always parallel to angular momentum surfaces and thus to surfaces of constant θ_e^*. Specification of the outflow temperature, T_{out}, as a function of θ_e^*, and determination of the radial distribution of θ_e in the boundary layer suffice to close the problem.

The outflow temperature, T_{out}, is defined as the absolute temperature along surfaces of constant θ_e^* as they

flare out to large radii in the upper portions of the vortex. It is clear from observations (e.g., Frank, 1977) that this occurs principally in the upper troposphere and lower stratosphere. The quantity of importance in determining the structure and amplitude is the mean outflow temperature weighted by $\ln\theta_e^*/\theta_{ea}$, as defined by (19). Thus the average outflow temperature is clearly weighted toward the upper portions of the outflow, where $\ln\theta_e^*/\theta_{ea}$ is relatively large. For simplicity we approximate $\bar{T}_{\text{out}}$ by a constant, T_0; a discussion of the effects of variable outflow temperature may be found in Lilly (unpublished manuscript).

We regard the main closure problem as that of determining the radial distribution of θ_e in the boundary layer. This is not an easy task, as the normal tropical boundary layer is far from thermodynamic equilibrium with the sea surface. Some understanding of the magnitude of this problem may be obtained by examining the distribution of θ_e in actual tropical cyclones, such as that presented by Hawkins and Imbembo (1976). Aside from prominent mesoscale fluctuations, the moist entropy of the boundary layer hardly increases inward until a radius of about twice the radius of maximum winds is attained. This is true despite the relatively strong winds (and presumably evaporation rates) evident well outside this region in their Fig. 16. This implies that the enhanced evaporation is largely compensated for by turbulent fluxes out of the boundary layer, at least in the outer regions of the tropical cyclone; these turbulent fluxes are most likely associated with cumulus convection. Simple boundary layer formulations that do not account for moist convective fluxes at the top of the boundary layer are thus not likely to produce accurate distributions of moist entropy in the boundary layer.

These limitations are clearly evident when one attempts a simple closure for the planetary boundary layer (PBL). An elegant closure for the tropical cyclone PBL was proposed by Ooyama (1969); we repeat a variation of his development here for completeness.

Consider the conservation equation for any conservative variable c assumed to be well-mixed in the vertical within a turbulent boundary layer of depth h. For steady axisymmetric flow, the rate equation for c is

$$u\frac{\partial c}{\partial r} = -\frac{\partial \tau_c}{\partial z}, \tag{27}$$

where u is the radial velocity and τ_c is the vertical flux of c by all processes excluding the mean axisymmetric circulation. Now the anelastic form of the mass continuity equation can be written

$$\frac{\partial}{\partial r}(\rho r u) + \frac{\partial}{\partial z}(\rho r w) = 0, \tag{28}$$

where ρ is density and w is the vertical velocity. A mass streamfunction ψ may be defined by virtue of (28), such that

$$\rho r u = -\partial\psi/\partial z. \tag{29}$$

Substituting (29) into (27) results in

$$\frac{\partial \psi}{\partial z}\frac{\partial c}{\partial r} = \rho r\frac{\partial \tau_c}{\partial z}. \tag{30}$$

Since density varies only slightly within the PBL and since c is assumed to be constant in z, (30) may be integrated in z to yield

$$\psi\left.\frac{\partial c}{\partial r}\right|_{z=h} = \rho_0 r[\tau_c|_{z=h} - \tau_c|_{z=0}], \tag{31}$$

where ρ_0 is a mean density in the boundary layer and we have made use of the boundary condition $\psi = 0$ on $z = 0$.

We now show that neglect of the flux terms at $z = h$ (the top of the boundary layer) leads to absurd predictions of the radial distribution of moist entropy in the PBL. We take as two conservative variables angular momentum M (although it may not be well mixed in the vertical) and moist entropy, s. If M and s are used for c in (34) and the resulting two equations are divided into each other, the result is

$$\left.\frac{\partial s}{\partial M}\right|_{z=h} = \left.\frac{\tau_s}{\tau_M}\right|_{z=0}. \tag{32}$$

The standard aerodynamic formulas are used for surface fluxes:

$$\left.\begin{aligned}\tau_s &= -C_p[C_\theta|V|(\ln\theta_e - \ln\theta_{es})]\\ \tau_M &= -C_D|V|rV\end{aligned}\right\}, \tag{33}$$

where $|V|$ is the magnitude of the surface horizontal velocity, C_θ and C_D are exchange coefficients for entropy and momentum, $\ln\theta_e$ and V are evaluated at the top of the mixed layer, and θ_{es} is the equivalent potential temperature of air saturated at sea surface temperature. If the relations (33) are substituted into (32), and $\partial s/\partial M$ is eliminated between (32) and (12), the result can be written

$$\ln\theta_e = \ln\theta_{es} - \frac{C_D}{C_\theta}\frac{1}{C_p(T_B - T_0)}\left(V^2 + \frac{1}{2}frV\right), \tag{34}$$

where (1) has been used for M. Note that for the steady vortex, C_D and C_θ do not enter separately but only as a ratio.

Since θ_{es} and V are functions of pressure and radius, (34) and (18) may be regarded as a closed set of relations for π and θ_e. Attempts to solve this set, however, lead to absurd radial distributions of velocity and temperature in the vortex. It is clear from (34) why this is so. For example, just outside the radius of maximum V in a reasonably strong vortex, the second term in parentheses in (34) is negligible compared to the first term since $V_{\max} > fr$; also V decreases rather sharply with radius in most observed tropical cyclones. Thus (34) would predict an *increase* of θ_e with radius in the region outside the radius of maximum winds but inside the radius where

$$-\frac{dV}{dr}=\frac{fV}{4V+fr}.$$

This is not only inconsistent with observations but, according to (32), implies that angular momentum must decrease with radius, a circumstance that would render the vortex inertially unstable.

Although the failure of the PBL formulation implied by (34) may be repaired by judicious tampering with the ratio of exchange coefficients or outflow temperature, it is far more likely, in view of observed distributions of θ_e, that the neglect of turbulent fluxes at the top of the PBL is the source of error. In particular, the import of low θ_e air into the boundary layer by turbulent entrainment and saturated downdrafts may constitute a significant part of the boundary layer θ_e budget (e.g., see Gray, 1982). It would appear from the observed θ_e distributions that in the outer regions of the tropical cyclone the sea surface evaporation is more nearly balanced by export through the top of the boundary layer than by the horizontal advection implied by the present treatment.

On the basis of the aforementioned arguments we formulate a semi-empirical boundary layer based on a division of the tropical cyclone boundary layer into three regions, as shown in Fig. 5. The innermost region, the eye, extends from the storm center out to the radius of the inner side of the eye wall. This region is mostly unsaturated and is probably mechanically controlled by the flow outside the eye. The second region extends from the inner eye wall to the radius of maximum winds and is assumed to be saturated on the cyclone scale. It is the only region of the cyclone that contains significant cyclone-scale vertical velocity. *We assume that in this second region, the great majority of the transport of θ_e through the top of the boundary layer is accomplished by the azimuthal and time mean circulation and that turbulent (nonaxisymmetric and nonsteady) fluxes through the top of the boundary layer are negligible.* Since the cyclone-scale vertical velocity keeps the air saturated there is virtually no entrainment of low-θ_e air from aloft in this region.

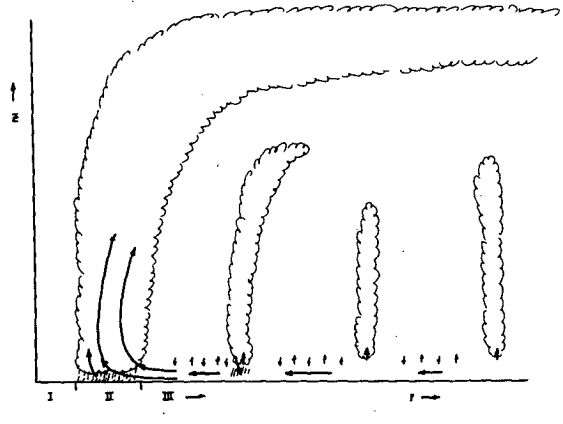

FIG. 5. Subdivision of the tropical cyclone boundary layer. Region I: the eye; Region II: the eyewall; Region III: the outer region. Considerable mixing of θ_e across the boundary layer top is assumed to occur in Region III. (See text.)

The third region extends from the radius of maximum winds to an outer radius r_0 and therefore covers most of the area of the storm. Ekman pumping is small (and at large radii negative) in this region due to relatively small vorticity; thus the time and azimuthal average vertical velocity is small. Following the arguments presented earlier in this section, we characterize this third region by vigorous turbulent exchange of θ_e through the top of the boundary layer. Here the total flux through the sea surface is balanced more by these turbulent fluxes than by horizontal advection. Obviously, treatment of this region requires more sophisticated physics, which account for turbulent entrainment, unsaturated downdrafts, etc. We must for the present regard a proper treatment of this third region as beyond the scope of this study; we turn instead to an empirical description based on composite thermodynamic analyses of observed tropical cyclones. Specifically, *we assume that the outer region of the tropical cyclone boundary layer is characterized by constant surface relative humidity* as suggested by composite analyses, such as that presented by Frank (1977).

In summary, we take the distribution of θ_e in the eye wall region to be dominated by cyclone scale fluxes while the region outside the radius of maximum winds is assumed to be controlled more by turbulent fluxes. As a first attempt to account for the core structure, we use Ooyama's formulation of the boundary layer there and in the eye as well. Based on observation, the outer region of the cyclone is simply assumed to be characterized by constant surface relative humidity.

In the outer region, the distribution of equivalent potential temperature is given by (25) with $\mathrm{RH}=\mathrm{RH}_a$:

$$\ln\frac{\theta_e}{\theta_{ea}}=-\ln\pi\left[1+\frac{Lq_a^*\mathrm{RH}_{as}}{RT_s}\right]. \tag{35}$$

When the above is substituted into (18) and the mean outflow temperature is approximated by T_0, the result may be written

$$\frac{1}{2}r\frac{\partial\ln\pi}{\partial r}+\beta\ln\pi=\frac{1}{4}\frac{f^2}{C_pT_B}(r_0^2-r^2)\quad\text{at}\quad z=h, \tag{36}$$

where

$$\beta\equiv 1-\epsilon\left(1+\frac{Lq_a^*\mathrm{RH}_{as}}{RT_s}\right), \tag{37}$$

and

$$\epsilon\equiv\frac{T_B-T_0}{T_B}. \tag{38}$$

When (36) is integrated once in r and the boundary condition $\ln\pi=0$ at $r=r_0$ is applied, the result is

$$\ln\pi=\frac{1}{4}\frac{f^2}{C_pT_B}\left[\frac{r_0^2}{\beta}-\frac{r^2}{1+\beta}-\frac{r_0^2}{\beta(1+\beta)}\left(\frac{r_0}{r}\right)^{2\beta}\right]. \tag{39}$$

Inside the radius of maximum wind, the distribution of pressure is determined by (34) together with (18) (with the outflow temperature set equal to T_0). In addition, we assume that in this region

$$fr \ll V$$

so that the last term on the right of (34) may be neglected and

$$V^2 \approx C_p T_B r \frac{\partial \ln \pi}{\partial r}.$$

With these approximations, θ_e may be eliminated between (34) and (18) to yield an equation for pressure alone:

$$\left(\frac{1}{2} - \frac{C_D}{C_\theta}\right) r \frac{\partial \ln \pi}{\partial r} + \left[1 - \epsilon\left(1 + \frac{Lq_a^*}{RT_s}\right)\right] \ln \pi = -\epsilon \ln \frac{\theta_{esa}}{\theta_{ea}} + \frac{1}{4} \frac{f^2}{C_p T_B} (r_0^2 - r^2) \quad \text{at} \quad z = h, \tag{40}$$

where θ_{esa} is the ambient saturation equivalent potential temperature at sea level. The solution to (40) is

$$\ln \pi = \ln \pi_{cs} + A r^\chi - \frac{1}{4} \frac{f^2 r^2}{C_p T_B \left[2 - \epsilon\left(1 + \frac{Lq_a^*}{RT_s}\right) - 2\frac{C_D}{C_\theta}\right]}, \tag{41}$$

where A is an integration constant, $\ln \pi_{cs}$ is given by (26) with $\mathrm{RH}_{cs} = 1$, and

$$\chi \equiv \frac{2\left[1 - \epsilon\left(1 + \frac{Lq_a^*}{RT_s}\right)\right]}{2\frac{C_D}{C_\theta} - 1}. \tag{42}$$

Clearly, the solution is only valid if $C_D/C_\theta > \frac{1}{2}$.

The inner solution (41) is valid out to the radius where RH has decreased to its ambient value. According to (25), this happens when

$$\ln \frac{\theta_e}{\theta_{ea}} = -\ln \pi \left[1 + \frac{Lq_a^* \mathrm{RH}_s}{RT_s}\right].$$

If this condition is applied to (40) and (18), we find that at the radius of maximum wind (where $\mathrm{RH}_s = \mathrm{RH}_{as}$)

$$V_{\max}^2 = \frac{C_\theta}{C_D} \epsilon L q_a^*(1 - \mathrm{RH}_{as}) \frac{1 - \frac{1}{4}\frac{f^2 r_0^2}{\beta R T_B}}{1 - \frac{1}{2}\frac{C_\theta}{C_D}\epsilon \frac{Lq_a^*(1 - \mathrm{RH}_{as})}{\beta R T_s}}, \tag{43}$$

$$\ln \pi = \frac{-\frac{1}{2}\epsilon \frac{C_\theta}{C_D}\frac{Lq_a^*}{C_p T_B}(1 - \mathrm{RH}_{as}) + \frac{1}{4}\frac{f^2 r_0^2}{C_p T_B}}{\beta - \frac{1}{2}\frac{C_\theta}{C_D}\epsilon \frac{Lq_a^*}{RT_s}(1 - \mathrm{RH}_{as})}, \tag{44}$$

where we have assumed that $f^2 r_{\max}^2 \ll 4RT_B$. Bear in mind that C_θ/C_D must be less than 2. Now the integration constant A in (41) can be found by requiring that (44) be satisfied at $r_{\max}$. Neglecting the last term on the right of (41), this condition may be written

$$A r_{\max}^\chi \approx \frac{\epsilon L q_a^*(1 - \mathrm{RH}_{as})\left(1 - \frac{1}{2}\frac{C_\theta}{C_D}\right)}{C_p T_s \beta}, \tag{45}$$

where we have also neglected the second term in the denominator of (44), which is about 5% of the first term. Finally, the outer solution given by (39) is matched to the inner solution given by (41), (42), and (45). Because of the form of (18), matching $\ln \pi$ automatically ensures that $d \ln \pi / dr$ is matched. This matching results in an explicit relationship between the outer radius r_0 and the radius $r_{\max}$ of maximum wind:

$$r_0^{2+2\beta} \approx r_{\max}^{2\beta} 2\epsilon \frac{C_\theta}{C_D}\frac{T_B}{T_S}\frac{Lq_a^*}{f^2}(1 - \mathrm{RH}_{as})(1 + \beta). \tag{46}$$

In summary, we have derived a solution for $\ln \pi$ under the condition that (34) applies to the cyclone core while the outer region of the cyclone is characterized by constant surface relative humidity. This solution is given by (39) outside $r_{\max}$ and (41) and (45) inside $r_{\max}$, with $r_{\max}$ related to r_0 by (46). The inner solution together with the cyclostrophic relation implies that

$$V \sim r^{\chi/2}, \tag{47}$$

with χ given by (42). The power law is sensitive to the ratio of the exchange coefficients for heat and momentum, with $\chi \approx 1$ for $C_D = C_\theta$. As it is likely that the inner region is not convectively neutral, (47) should not be taken seriously in region I. Just outside of $r_{\max}$, (39) implies that

$$V \sim r^{-\beta}. \tag{48}$$

For typical values of sea surface and tropopause temperatures, $\beta \approx 0.5$ so that (48) is close to the observed minus one-half power law typical of tropical cyclones.

The maximum azimuthal gradient wind given by (43) is plotted in Fig. 6 for conditions identical to those assumed in constructing Fig. 2 and with $C_D = C_\theta$. Maximum gradient winds of about 75 m s^{-1} are achieved for high surface air temperature and very low outflow temperature. The outer radius given by (46) is shown in Fig. 7 as a function of radius of maximum winds, surface air temperature and outflow temperature for $C_D = C_\theta$. The conditions assumed are the same as those for Figs. 2 and 6. The following conclusions may be drawn from (46) and from Fig. 7:

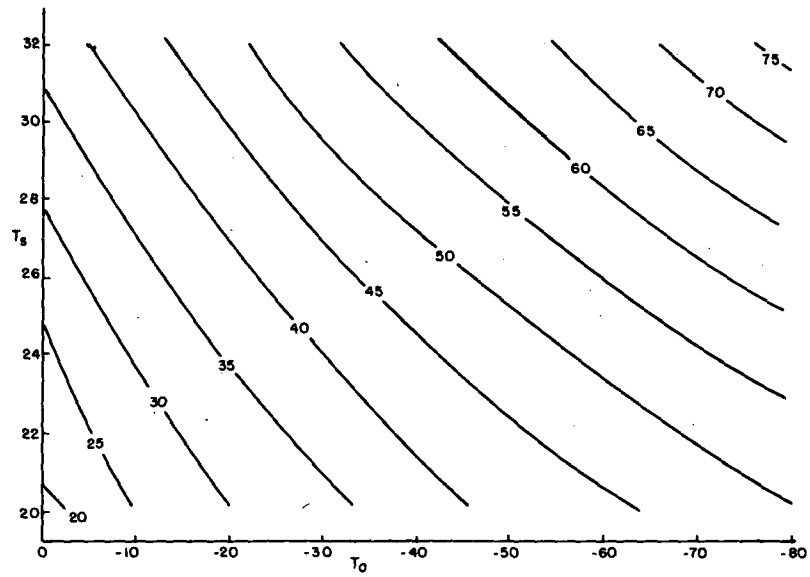

FIG. 6. Maximum gradient wind (m s^{-1}) as a function of surface air temperature (T_s, °C) and outflow temperature (T_0, °C) computed from (43) for the same conditions as used to construct Fig. 2 and $C_e = C_D$.

1) As latitude increases the outer radius becomes smaller and/or the radius of maximum winds becomes larger.

2) As sea surface temperature increases the outer radius increases and/or the radius of maximum winds decreases.

3) As the outflow temperature decreases the outer radius increases and/or the radius of maximum winds decreases.

4) Due to the dependence of steady-state tropical cyclone intensity on sea surface and outflow temperatures, the ratio of the radius of maximum winds to the outer radius decreases with increasing steady-state intensity.

We stress that neither the core radius nor the outer radius are directly related to intensity [except for the effect of outer radius on intensity evident in (26)]; rather their ratio should be related to latitude, sea surface temperature and outflow temperature in the mature tropical cyclone. This constitutes an observationally testable hypothesis.

d. Two-dimensional structure of the steady tropical cyclone

By coupling the interior vortex solution described by (18) with a boundary layer such as that developed in the preceding section, we have shown that it is possible to obtain radial distributions of quantities at the top of the boundary layer which conform at least roughly with observations. The complete two-dimensional structure of the steady tropical cyclone now can be obtained easily by evaluating quantities along angular momentum surfaces, whose shape above the boundary layer is given by (11). The latter, for convenience, is rewritten

$$r^2|_M = r_B{}^2|_M \frac{T_B - T_{\text{out}}}{T - T_{\text{out}}}, \tag{49}$$

where $r_B{}^2$ is the radius of a particular M surface where it intersects the top of the boundary layer. Although we have heretofore approximated T_{out} by the constant T_0, the same approximation introduces an error in (49) that, while small at $z = h$, may become large near the tropopause. In evaluating (49), therefore, we expand the actual variation of T_{out} about its mean value T_0:

$$T_{\text{out}}(s^*) = T_0 + \left.\frac{dT}{ds^*}\right|_{T_0} (s^* - s_a^*) = T_0 - T_0\gamma \ln \frac{\theta_e^*}{\theta_{ea}}, \tag{50}$$

where

$$\gamma \equiv -\frac{1}{-T_0} \left.\frac{dT}{d \ln\theta_e^*}\right|_{T_0}.$$

Substituting the above into (49) gives

$$r^2|_M = r_B{}^2|_M \frac{T_B - T_0 + T_0\gamma \ln \dfrac{\theta_e^*}{\theta_{ea}^*}}{T - T_0 + T_0\gamma \ln \dfrac{\theta_e^*}{\theta_{ea}^*}}. \tag{51}$$

We use (51) to directly infer the radius of M and θ_e^* surfaces as a function of temperature above the boundary layer.

As a matter of convenience, the height of the M surfaces may be obtained by noting that the constancy

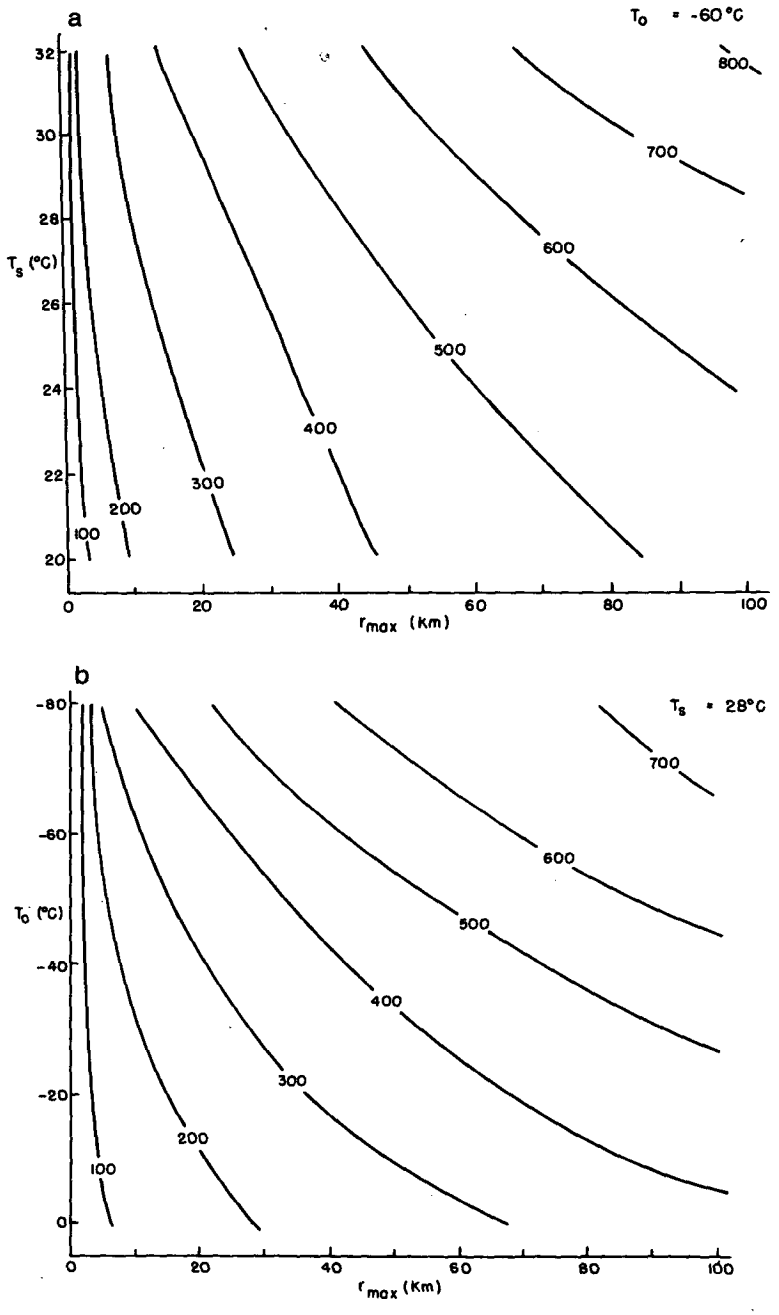

FIG. 7. (a) Outer radius r_0 (km) as a function of radius of maximum winds, r_{max} (km) and surface air temperature T_s, computed from (46) for $T_0 = -60°C$ and conditions otherwise the same as those used in constructing Fig. 6. (b) As in (a) except showing r_0 as a function of r_{max} and T_0.

of θ_e^* along M surfaces implies that the saturated moist static energy, defined

$$h^* \equiv C_pT + gz + Lq^* \tag{52}$$

is approximately constant along such surfaces. Since q^* is a function of temperature and pressure, we must also find the pressure distribution along M surfaces in order to infer the height of the surfaces from (52). To do this, we use a simple and rapidly converging iterative procedure. First, a value of π is guessed for a point characterized by a particular temperature along a particular M surface. [The radius of that point is found using (51).] The saturation mixing ratio is then found from the Clausius-Clapeyron equation using the guessed value of π:

$$q^* = q^*|_{z=h}\left(\frac{\pi|_{z=h}}{\pi}\right)^{c_p/R} \exp\left[\frac{L}{R_v}\left(\frac{1}{T|_{z=h}} - \frac{1}{T}\right)\right], \quad (53)$$

where R_v is the gas constant for water vapor. Next, the potential temperature is found by inverting the definition of θ_e^*:

$$\theta = \theta_e^* \exp(-Lq^*/C_pT). \quad (54)$$

Finally, a new value of π is found from T and θ:

$$\pi = T/\theta. \quad (55)$$

This new value of π is then used as a new estimate and the procedure starting with (53) is repeated. After only a few iterations, accurate values of q^*, θ, and π are found. Finally, the height z is obtained from (52):

$$z = \frac{C_p}{g}(T_B - T) + \frac{L}{g}(q^*|_{z=h} - q^*). \quad (56)$$

The azimuthal velocity is easily found by solving (1) for V.

As an example of the two-dimensional structure derived as described above, we use the relations (18) (with $T_{out} = T_0$) together with the boundary layer model discussed in Section 2c to arrive at the radial distribution of variables at the top of the boundary layer. The distributions along M surfaces are then derived using the aforementioned procedure. The vortex is calculated for the following conditions: $T_s = 27°C$, $T_B = 22°C$, $T_0 = -67°C$, f evaluated at 28° latitude, $p_0 = 1015$ mb, $r_0 = 400$ km, $C_\theta = C_D$, $RH_a = 80\%$, and $\gamma = 2$ (corresponding to a Brunt-Väisälä frequency of 1.5×10^{-2} s^{-1}). Under these conditions the central pressure is 941 mb, the maximum gradient wind is 58 m s^{-1}, the radius of maximum winds is 35.8 km, the ambient boundary layer θ_e is 349 K, $\epsilon = 0.3$, $\beta = 0.542$, and $\chi = 0.502$.

The distributions of M, θ_e^*, V, and temperature perturbation from the base state, T', are shown in the r–z plane in Figs. 8–11. The major observed features are well represented in the analytic solution. These include the warm core centered at high altitude, the outward sloping velocity maximum, and the strong radial gradient of θ_e^* near and inside the velocity maximum. The radial distribution of V inside the velocity maximum, showing a near $r^{1/2}$ dependence, does not agree with the observations of near solid body rotation. We do not claim to have accurately described the eye region where noncyclostrophic processes play an important role (Smith, 1980; Pearce, 1981). The overall structure and magnitude of the disturbance is realistic, however, and we feel that this supports our contention that ambient conditional instability is not needed for cyclone maintenance over warm water.

e. *Boundary layer radial and vertical velocities*

Estimates of the streamfunction at the top of the boundary layer may be made by assuming that Ooyama's boundary layer formulation (31) gives the correct momentum balance in the boundary layer without considering turbulent fluxes at the top of the layer, even if neglect of the latter yields an incorrect heat budget. If we take angular momentum as the conservative quantity in (31), the latter, taken together with surface stress given by (33), may be solved for the streamfunction. The vertical velocity is then related to the streamfunction by

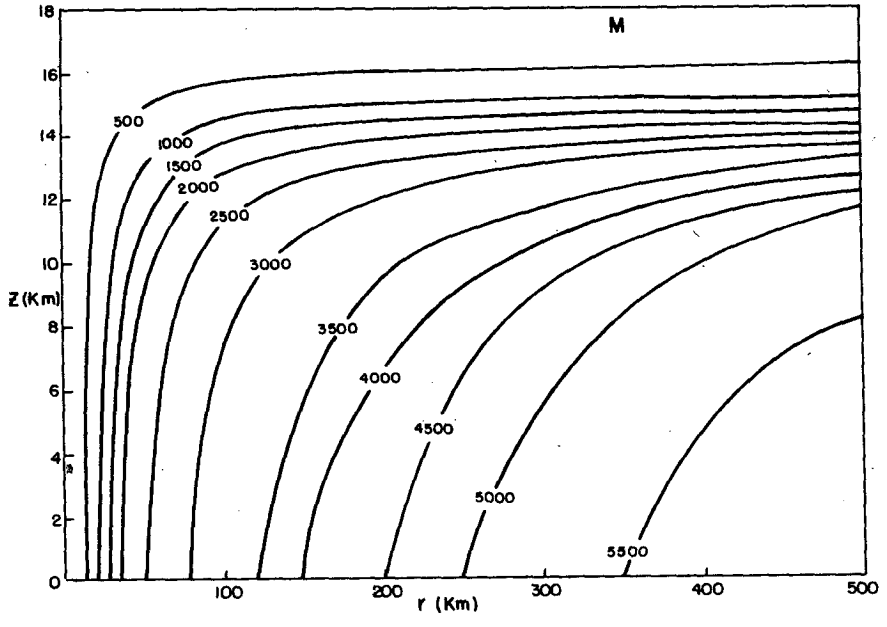

FIG. 8. Distribution of absolute angular momentum (10^3 m^2 s^{-1}) in the vortex discussed in Section 2d.

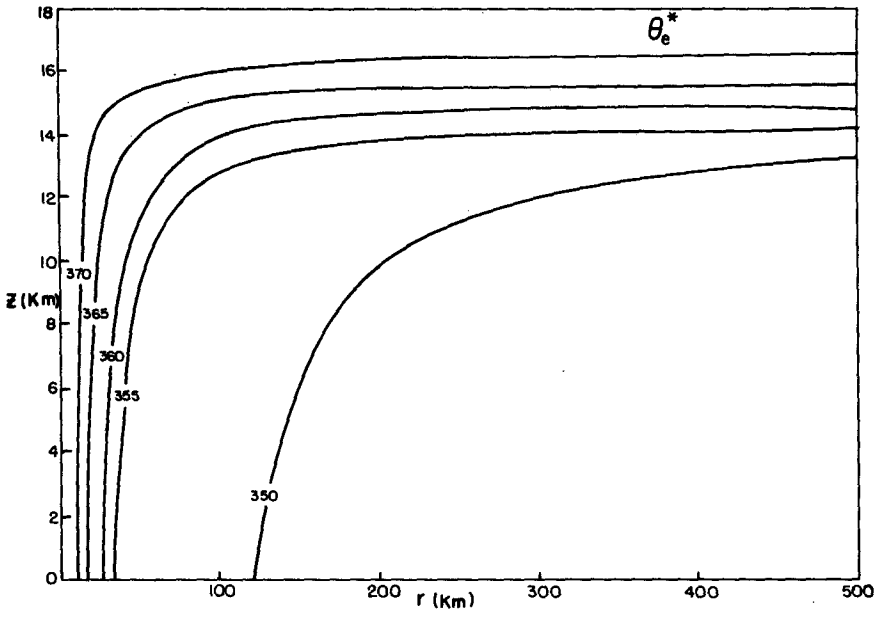

FIG. 9. As in Fig. 8 but for saturation equivalent potential temperature (°K).

$$\rho r w = \partial\psi/\partial r,$$

while the radial velocity is given by (29). The mean radial velocity in the boundary layer may be found by integrating (29) across the depth of the layer, so that

$$r\bar{u} = -\frac{1}{\rho h}\psi,$$

where h is the nominal depth of the layer and ρ is the mean density. Figure 12 shows the radial distribution of vertical velocity at the top of the boundary layer and mean radial velocity within the layer as a function of radius for the vortex described in section 2d. For the purpose of calculating these quantities, we have taken ρ and h to be constant, with $h = 1$ km. The drag coefficient is assumed constant with a value of 2×10^{-3}.

The distributions shown in Fig. 12 are for the most part reasonable, with the vertical velocity showing a sharp peak at the radius of maximum winds and the radial velocity reaching a maximum at much larger radii. The streamfunction has a discontinuity at r_{max} as a consequence of matching two separate boundary

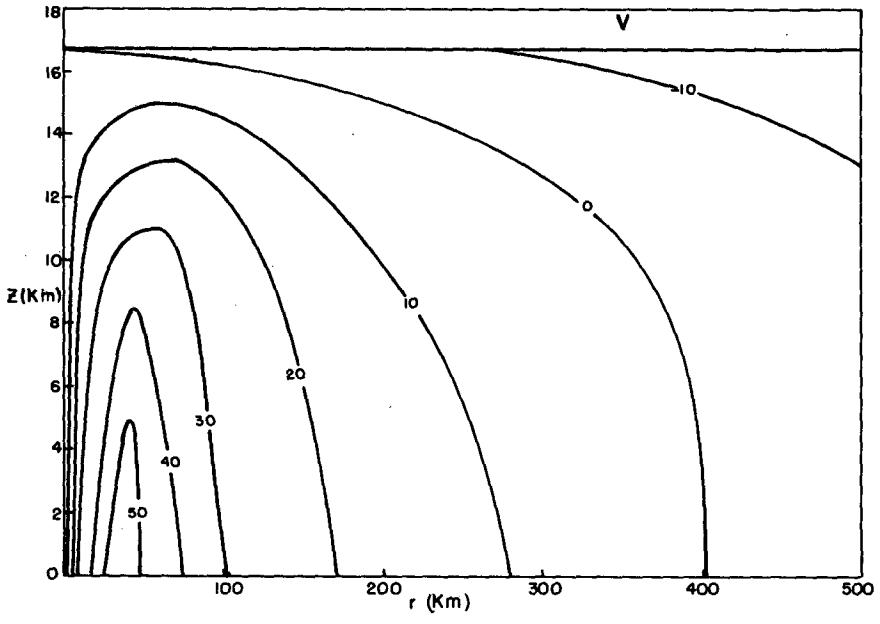

FIG. 10. As in Fig. 8 but for gradient wind (m s^{-1}).

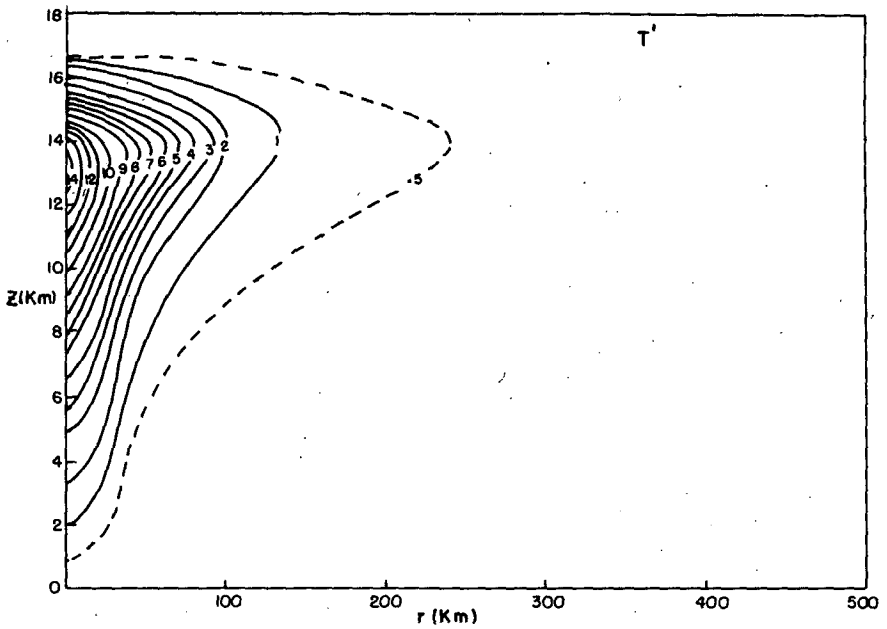

FIG. 11. As in Fig. 8 but for temperature departure (°C) from far environment at same altitude.

layers there, since the radial gradient of angular momentum is discontinuous. This results in a jump in u and a delta function spike of vertical velocity at r_{max}. These unrealistic features would not be present had a single boundary layer representation been applied throughout the vortex.

3. The tropical cyclone as a Carnot heat engine

The preceding results suggest that the steady tropical cyclone may be regarded as a simple Carnot heat engine in which air flowing inward in the boundary layer acquires moist entropy from the sea surface, ascends, and ultimately gives off heat at the much lower temperature of the lower stratosphere or upper troposphere. A schematic of the heat engine is shown in Fig. 13. Air begins to flow inward at constant temperature along the lower boundary at radius r_0 and acquires an incremental latent heat

$$\Delta Q_1 = \int_{\theta_{ea}}^{\theta_e} C_p T_B d \ln\theta_e = C_p T_B \ln \frac{\theta_e}{\theta_{ea}}, \qquad (57)$$

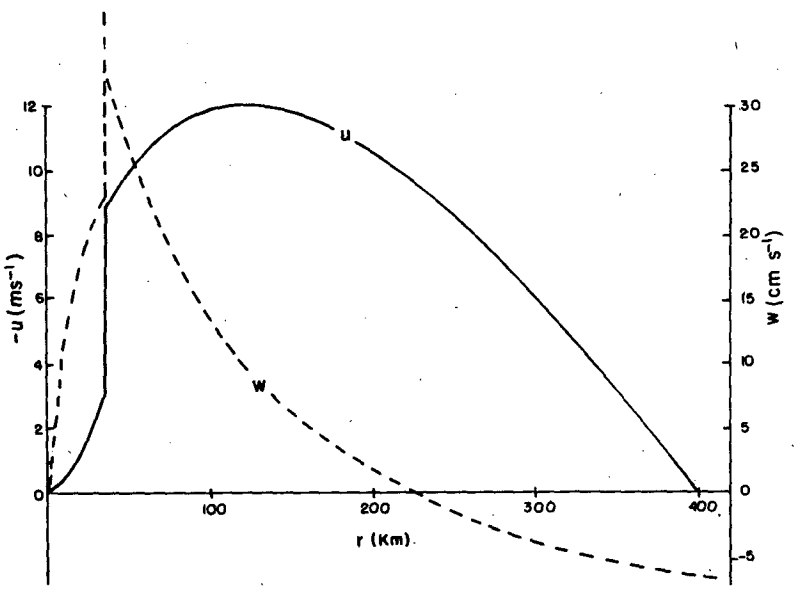

FIG. 12. Radial distribution of vertical velocity (cm s^{-1}) at the top of the boundary layer, and mean radial velocity (m s^{-1}) within the boundary layer of the vortex discussed in Section 2e.

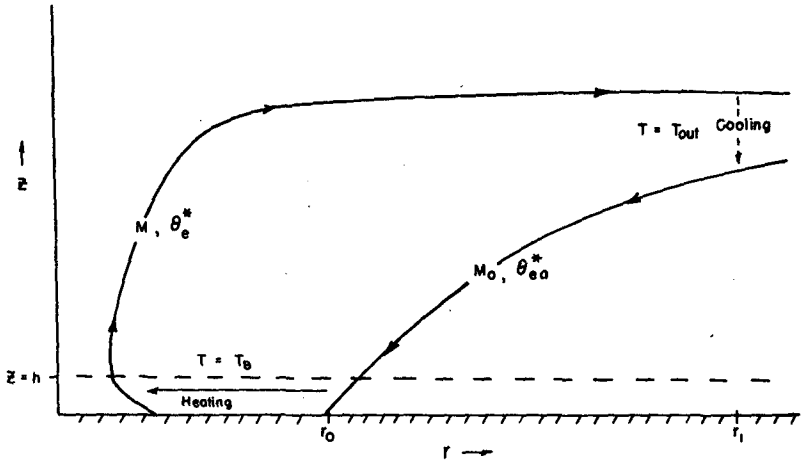

FIG. 13. The tropical cyclone as a Carnot heat engine. See text for explanation.

where θ_{ea} is the equivalent potential temperature at r_0. The air ascends at constant entropy along an M surface and flows out to large radius. To complete the circuit, the air eventually loses enough total heat through radiational cooling to return to its ambient θ_e so that

$$\Delta Q_2 = \int_{\theta_e}^{\theta_{ea}} C_p T_{\text{out}} d\ln\theta_e = -C_p \bar{T}_{\text{out}} \ln\frac{\theta_e}{\theta_{ea}}, \quad (58)$$

where $\bar{T}_{\text{out}}$ is given by (19). The total heating, from (57) and (58), is therefore

$$\Delta Q = \Delta Q_1 + \Delta Q_2 = C_p T_B \epsilon \ln\frac{\theta_e}{\theta_{ea}}, \quad (59)$$

where $\epsilon \equiv (T_B - \bar{T}_{\text{out}})/T_B$ is the thermodynamic efficiency. This net heating is used to do work against frictional dissipation in the steady tropical cyclone. Referring to Fig. 13, it is seen that work is done against friction in the inflowing boundary layer air and also to change the angular momentum back to its ambient value at large radii in the outflow. Kinetic energy is also dissipated by turbulence within cumulus clouds; however, we hold that this sink primarily balances kinetic energy generated by release of the ambient convective available potential energy as is probably the case in the unperturbed tropical atmosphere. This is simply a statement that convective clouds in tropical cyclones are locally similar to those away from such disturbances.

The balance between total heating and frictional dissipation in the inflow and outflow may be written symbolically

$$\Delta Q = W_{\text{PBL}} + W_0, \quad (60)$$

where W_{PBL} and W_0 are the work done in the boundary layer and outflow, respectively. The latter is simply proportional to the change in kinetic energy needed to bring the angular momentum of the outflow, M, back to its ambient value M_0:

$$W_0 = \frac{1}{2}\Delta V^2 = \frac{1}{2}\left[\left(\frac{M}{r_1} - \frac{1}{2}fr_1\right)^2 - \left(\frac{M_0}{r_1} - \frac{1}{2}fr_1\right)^2\right]$$

$$= \frac{1}{2}\left[\frac{M^2 - M_0^2}{r_1^2} + f(M_0 - M)\right], \quad (61)$$

where we have related azimuthal velocity to angular momentum using (1) and r_1 is some large radius at which the exchange takes place. In the limit of large r_1,

$$\lim_{r_1\to\infty} W_0 = \frac{1}{2}f(M_0 - M) = \frac{1}{4}f^2(r_0^2 - r^2) - \frac{1}{2}frV. \quad (62)$$

Using the above and (59) and (60) we infer the work done in the boundary layer:

$$W_{\text{PBL}} = C_p T_B \epsilon \ln\frac{\theta_e}{\theta_{ea}} + \frac{1}{2}frV - \frac{1}{4}f^2(r_0^2 - r^2). \quad (63)$$

Finally, knowledge of the work done against dissipation in the boundary layer allows an evaluation of the pressure distribution in the boundary layer through the use of Bernoulli's equation. The latter, when integrated inward from r_0 at constant temperature, may be written

$$\frac{1}{2}V^2 + C_p T_B \ln\pi + W_{\text{PBL}} = 0 \quad \text{at} \quad z = 0. \quad (64)$$

When (63) is substituted into this and the gradient wind equation is used for the sum $V^2 + frV$, the result is

$$\ln\pi + \frac{1}{2}r\frac{\partial \ln\pi}{\partial r} + \epsilon \ln\frac{\theta_e}{\theta_{ea}} - \frac{1}{4}\frac{f^2}{C_p T_B}(r_0^2 - r^2) = 0$$

$$\text{at} \quad z = 0, \quad (65)$$

which is identical to (18). This confirms the interpretation of the results of the previous section in terms of a Carnot engine.

Note that if heat is removed and angular momentum added to the outflow at some finite radius r_1, inspection of (61) shows that the work needed to increase the angular momentum of the outflow is less than the case of infinite r_1 and more thermal energy is available to overcome friction in the inflow. This suggests a stronger cyclone. Substitution of the full form of (61) into (63), combining the result with (59) and (64), and using (25), shows that the central pressure is decreased by an amount given by

$$\delta \ln \pi = \frac{-\frac{1}{8}\frac{f^2 r_0^4}{r_1^2}}{C_p T_B\left[1-\epsilon\left(1+\frac{Lq_a^* \mathrm{RH}_s}{RT_s}\right)\right]}.$$

Even when $r_1 = r_0$, this is quantitatively insignificant unless r_0 is very large.

4. Conclusions

It has long been recognized that the transfer of latent heat from the ocean to the atmosphere is extremely important in the development and maintenance of tropical cyclones. But since nearly all numerical simulations to date have used initial thermodynamic soundings that show some conditional instability, the role of the latter in tropical cyclone development and maintenance has not been clearly separated from the role of the oceanic heat source. We have attempted to show here that tropical cyclones can be maintained in an intense steady state without any contribution from ambient conditional instability. Energetically, our model resembles a simple Carnot heat engine in which latent and sensible heat are extracted from the ocean at a temperature T_B and ultimately given up in the outflow at a temperature T_{out}. The thermodynamic efficiency of the engine is therefore $(T_B - T_{out})/T_B$. This efficiency, multiplied by the oceanic heat source, represents the production of energy which is used to overcome frictional dissipation in the boundary layer and at large radii in the outflow. Although this view explicitly neglects ambient conditional instability, some must be present to overcome dissipation within cumulus clouds. In addition, the depth of the ambient neutral or unstable layer must be sufficient to assure that the outflow from the cyclone is cold enough to account for a reasonable thermodynamic efficiency. In our view, the absence of tropical cyclone development when the sea water temperature is less than about 26°C is related to the circumstance that the depth of the conditionally neutral or unstable layer is usually too shallow under these conditions to allow a reasonable thermodynamic efficiency.

The steady, axisymmetric model presented here consists of two parts. The first is used to represent the flow above the boundary layer, and assumes that this flow is in hydrostatic and gradient wind balance. In addition, the saturated moist entropy is assumed constant along angular momentum surfaces so that the vortex is exactly neutral to slantwise moist convection of boundary layer air. These assumptions lead to an explicit relationship (18) between moist entropy and angular momentum at the top of the boundary layer and can be used by itself to predict the central pressure of the cyclone as a function of core surface relative humidity. Although the assumption of moist neutrality breaks down in the eye itself, the prediction of minimum attainable central pressure by this model is in reasonable accord with observations, perhaps because the overestimate of θ_e made by assuming saturation at sea level tends to compensate the lack of subsidence warming. The model suggests that extremely intense cyclones would occur were sea surface temperatures substantially warmer or stratospheric temperatures much colder than at present.

The second part of the model, discussed in section 2c, describes the boundary layer and is used to make a second prediction of the relationship between moist entropy and angular momentum at its top. When coupled with the interior vortex, all properties of the two-dimensional steady vortex are predicted. However, if one assumes a simple balance between horizontal advection and sea surface fluxes of angular momentum and moist entropy, the latter is predicted to increase inward much more rapidly than observed. We conclude that turbulent exchange of θ_e at the top of the boundary layer is a critical component of the heat budget outside the core of the cyclone, as has been found in previous investigations. Lacking a better idea, we make use of the empirical observation that the relative humidity outside the core is nearly constant. Inside the radius of maximum winds we assume that surface fluxes balance horizontal advection. Matching the core boundary layer to the outer boundary layer closes the problem and produces an explicit relationship between the radius of maximum winds and the outer radius r_0. The magnitude and structure of the vortex calculated this way seem quite realistic, except in the eye itself.

Neither the boundary layer physics nor the dynamics of the eye have been properly accounted for in this study. Lateral mixing of heat, water and momentum between the eye and the eye wall are thought to have important consequences for the structure and dynamics of the eye (Malkus, 1958), but these processes are neglected here. In spite of these deficiencies, the present work strongly suggests that ambient conditional instability plays at most a secondary role in tropical cyclone maintenance. This point leaves open the question of whether the *initial spin-up* of the cyclone is due more to the organized release of ambient conditional instability or to anomalous sea surface fluxes. These unsteady and turbulent aspects of tropical cyclone dynamics are not particularly amenable to analytic treatment but may be studied using numerical models, especially when a simple model such as the one presented here is used to provide specific hypotheses to test with the numerical model. The investigation of

some of these properties of tropical cyclones using numerical experimentation will be the subject of Part II.

Acknowledgments. The author gratefully acknowledges the fruitful exchange of ideas with Dr. Douglas Lilly of Oklahoma University, which led to many improvements in this work. During the course of this investigation, the author discovered that Dr. Lilly had worked out many of the salient features of this analysis several years earlier. As we arrived at some of the same conclusions independently and since our views diverge with respect to some of the details, we have elected to jointly publish independent papers. I am also grateful for numerous enlightening exchanges with Richard Rotunno, Roger Smith, Bruce Morton, Greg Holland, and William Gray. This work was supported in part by National Science Foundation Grant ATM-8313454.

APPENDIX I

An Elementary Relation of Moist Thermodynamics

In a saturated atmosphere it is possible to define a saturated moist entropy, s^*, which is invariant under moist reversible processes. This quantity satisfies a modified form of the first law of thermodynamics:

$$Tds^* = du + pd\alpha - Ldq^*, \tag{A1}$$

where u is the internal energy, L is the heat of vaporization, and q^* is the saturation mixing ratio. It is also possible to define a saturated moist enthalpy h^* such that

$$h^* \equiv u + p\alpha - Lq^*. \tag{A2}$$

From (A1) and (A2) it follows that

$$dh^* = Tds^* + \alpha dp. \tag{A3}$$

From this it may be deduced that

$$(\partial h^*/\partial p)_{s^*} = \alpha, \tag{A4}$$

$$(\partial h^*/\partial s^*)_p = T. \tag{A5}$$

Now, because q^* is a function of temperature and pressure alone, h^* is a state variable which may be expressed as a function of any other two state variables, such as p and s^*. Thus

$$\left(\frac{\partial}{\partial s^*}\right)_p\left(\frac{\partial h^*}{\partial p}\right)_{s^*} = \left(\frac{\partial}{\partial p}\right)_{s^*}\left(\frac{\partial h^*}{\partial s^*}\right)_p.$$

Substituting (A4) and (A5) into the above we obtain

$$\left(\frac{\partial \alpha}{\partial s^*}\right)_p = \left(\frac{\partial T}{\partial p}\right)_{s^*}, \tag{A6}$$

which is the desired result.

APPENDIX II

Saturated Equivalent Potential Vorticity in the Eye

It is possible to show that to a close approximation, M and s^* surfaces are parallel in the eye even though s^* above the boundary layer may be much larger than s within the boundary layer. This will be true to the extent that the eye is in solid body rotation.

Suppose that the eye is bounded by an M surface, M_w, which lies at a radius $r_w(p)$ that is everywhere within the region where slantwise neutrality applies. Then the M_w surface corresponds to a saturated moist entropy surface s_w^*. If at each pressure level within the eye the azimuthal velocity is approximately linear in r, then

$$M^2 = {M_w}^2\left(\frac{r}{r_w(p)}\right)^4. \tag{B1}$$

If in addition, hydrostatic and gradient wind balance obtain in the eye then the thermal wind relation (8) applies and may be written using (B1)

$$\frac{1}{r^3}\left(\frac{\partial M^2}{\partial p}\right)_r = \frac{-4{M_w}^2 r}{{r_w}^5(p)}\frac{\partial r_w}{\partial p} = -\left(\frac{\partial T}{\partial p}\right)_{s^*}\left(\frac{\partial s^*}{\partial r}\right)_p. \tag{B2}$$

Now since the bounding M surface lies within the region of slantwise neutrality, (10) applies there and may be written

$$\frac{\partial r_w}{\partial p} = \frac{{r_w}^3}{2M_w}\left(\frac{ds^*}{dM}\right)_{r_w}\left(\frac{\partial T}{\partial p}\right)_{s^*,r_w}. \tag{B3}$$

Substituting the above into (B2) yields

$$\left(\frac{\partial s^*}{\partial r}\right)_p\left(\frac{\partial T}{\partial p}\right)_{s^*} = \frac{2M_w}{{r_w}^2}r\left(\frac{ds^*}{dM}\right)_{r_w}\left(\frac{\partial T}{\partial p}\right)_{s^*,r_w}. \tag{B4}$$

But from (B1) we have

$$\frac{\partial M}{\partial r} = \frac{2M_w}{{r_w}^2}r,$$

so that (B4) may be written

$$\left(\frac{\partial s^*}{\partial r}\right)_p\left(\frac{\partial T}{\partial p}\right)_{s^*} = \frac{\partial M}{\partial r}\left(\frac{ds^*}{dM}\right)_{r_w}\left(\frac{\partial T}{\partial p}\right)_{s^*,r_w}. \tag{B5}$$

Now if we regard s^* in the eye as a function of both M and p, then (B5) becomes

$$\left(\frac{\partial s^*}{\partial M}\right)_p\left(\frac{\partial T}{\partial p}\right)_{s^*} = \left(\frac{ds^*}{dM}\right)_{r_w}\left(\frac{\partial T}{\partial p}\right)_{s^*,r_w}. \tag{B6}$$

Since $(ds^*/dM)_{r_w}$ is a constant, the quantity $(\partial s^*/\partial M)_p$ in the eye will, from (B6), be proportional to

$$\frac{(\partial T/\partial p)_{s^*,r_w}}{(\partial T/\partial p)_{s^*}}, \tag{B7}$$

which is the ratio of moist adiabatic lapse rate at a given pressure level in the eye wall to the lapse rate at the same pressure level within the eye. To the extent that this ratio is only a function of M in the eye, the quantity $(\partial s^*/\partial M)_p$ will vary only with M so that s^* and M surfaces will coincide. The ratio (B7) will in fact vary somewhat along M surfaces; the author has calculated about a 7% change in the extreme case of a

storm with 900 mb central pressure and eye wall surface pressure of 930 mb. Thus to a good approximation, s^* and M surfaces coincide within the eye if the latter is in solid body rotation and bounded by an eye wall which is neutral to slantwise moist convection. This is confirmed by the observation of near moist-adiabatic temperature lapse rates above 800 mb in the eyes of hurricanes (Jordan, 1957).

REFERENCES

Anthes, R. A., 1972: Non-developing experiments with a three-level axisymmetric hurricane model. NOAA Tech. Mem. ERL NHRL-97, 18 pp.

——, 1982: *Tropical Cyclones: Their Evolution, Structure, and Effects, Meteor. Monogr.*, No. 41, Amer. Meteor. Soc., 208 pp.

Arakawa, A., and W. H. Schubert, 1974: Interaction of a cumulus cloud ensemble with the large-scale environment, Part I. *J. Atmos. Sci.*, **31**, 674–701.

Carrier, G. F., A. L. Hammond and O. D. George, 1971: A model of the mature hurricane. *J. Fluid Mech.*, **47**, 145–170.

Charney, J. G., and A. Eliassen, 1964: On the growth of the hurricane depression. *J. Atmos. Sci.*, **21**, 68–75.

DeMaria, M., and W. H. Schubert, 1984: Experiment with a spectral tropical cyclone model. *J. Atmos. Sci.*, **41**, 901–924.

Emanuel, K. A., 1983: On assessing local conditional symmetric instability from atmospheric soundings. *Mon. Wea. Rev.*, **111**, 2016–2033.

——, 1985: Frontal circulation in the presence of small moist symmetric stability. *J. Atmos. Sci.*, **42**, 1062–1071.

Frank, W. M., 1977: The structure and energetics of the tropical cyclone I. Storm structure. *Mon. Wea. Rev.*, **105**, 1119–1135.

Gray, W. M., 1982: Tropical cyclone genesis and intensification. *Intense Atmospheric Vortices*, L. Bengtsson and J. Lighthill, Eds., Springer-Verlag, 3–20.

Hawkins, H. F., and S. M. Imbembo, 1976: The structure of a small, intense hurricane—Inez 1966. *Mon. Wea. Rev.*, **104**, 418–442.

Hoskins, B. J., M. E. McIntyre and A. W. Robertson, 1985: On the use and significance of isentropic potential-vorticity maps. *Quart. J. Roy. Meteor. Soc.*, **111**, 877–946.

Jordan, C. L., 1957: Mean soundings for the hurricane eye. Natl. Hurricane Res. Proj. Rep. No. 13, U.S. Dept. of Commerce. 10 pp.

——, 1958: Mean soundings for the West Indies area. *J. Meteor.*, **15**, 91–97.

Lord, S. J., H. E. Willoughby and J. M. Piotrowicz, 1984: Role of parameterized ice-phase microphysics in an axisymmetric, nonhydrostatic tropical cyclone model. *J. Atmos. Sci.*, **41**, 2836–2848.

Malkus, J. S., 1958: On the structure and maintenance of the mature hurricane eye. *J. Meteor.*, **15**, 337–349.

——, and H. Riehl, 1960: On the dynamics and energy transformations in steady-state hurricanes. *Tellus*, **12**, 1–20.

Newell, R. E., J. W. Kidson, P. G. Vincent and G. J. Boer, 1972: *The General Circulation of the Tropical Atmosphere. Vol. 1.*, MIT Press.

Ooyama, K., 1964: A dynamical model for the study of tropical cyclone development. *Geofys. Int.*, **4**, 187–198.

——, 1969: Numerical simulation of the life cycle of tropical cyclones. *J. Atmos. Sci.*, **26**, 3–40.

——, 1982: Conceptual evolution of the theory and modeling of the tropical cyclone. *J. Meteor. Soc. Japan*, **60**, 369–379.

Pearce, R. P., 1981: A dynamical analysis of hurricane intensification. *Contrib. Atmos. Phys.*, **54**, 19–42.

Price, J. F., 1981: Upper ocean response to a hurricane. *J. Phys. Oceanogr.*, **11**, 153–175.

Reynolds, R. W., 1982: A monthly climatology of sea surface temperature. NOAA Tech. Rep. NWS 31.

Riehl, H., 1963: Some relations between wind and thermal structure of steady state hurricanes. *J. Atmos. Sci.*, **20**, 276–287.

——, 1954: *Tropical Meteorology*. McGraw-Hill, 392 pp.

Schubert, W. H., and J. J. Hack, 1983: Transformed Eliassen-balanced vortex model. *J. Atmos. Sci.*, **40**, 1571–1583.

Smith, R. K., 1980: Tropical cyclone eye dynamics. *J. Atmos. Sci.*, **37**, 1227–1232.

Thorpe, A. J., 1985: Diagnosis of a balanced vortex using potential vorticity. *J. Atmos. Sci.*, **42**, 397–406.

Tuleya, R. E., and Y. Kurihara, 1981: A numerical study of the effects of environmental flow on tropical storm genesis. *Mon. Wea. Rev.*, **109**, 2487–2506.